High-Pressure Synthesis, Crystal Structures, and Properties of Perovskite-like $BiAlO_3$ and Pyroxene-like $BiGaO_3$

Alexei A. Belik,*,† Tuerxun Wuernisha,‡ Takashi Kamiyama,‡ Kazuhiro Mori,§ Makoto Maie,|| Takuro Nagai,⊥ Yoshio Matsui,|| and Eiji Takayama-Muromachi||

International Center for Young Scientists (ICYS), High Voltage Electron Microscopy Station (HVEMS), and Advanced Materials Laboratory (AML), National Institute for Materials Science (NIMS), 1-1 Namiki, Tsukuba, Ibaraki 305-0044, Japan, Research Reactor Institute, Kyoto University, Kumatori-cho, Osaka 590-0494, Japan, and Institute of Materials Structure Science, High Energy Accelerator Research Organization (KEK), 1-1 Oho, Tsukuba, Ibaraki 305-0801, Japan

Received September 7, 2005. Revised Manuscript Received October 30, 2005

New oxides, $BiAlO_3$ and $BiGaO_3$, were prepared using a high-pressure high-temperature technique at 6 GPa and 1273−1473 K. $BiAlO_3$ is isotypic with multiferroic perovskite-like $BiFeO_3$ and has octahedrally coordinated Al^{3+} ions. Structure parameters of $BiAlO_3$ were refined from laboratory X-ray powder diffraction data (space group *R*3*c*; $Z = 6$; $a = 5.37546(5)$ Å and $c = 13.3933(1)$ Å). $BiGaO_3$ has the structure closely related to pyroxene-like KVO_3. Structure parameters of $BiGaO_3$ were refined from time-of-flight neutron powder diffraction data (space group *Pcca*; $Z = 4$; $a = 5.4162(2)$ Å, $b = 5.1335(3)$ Å, and $c = 9.9369(5)$ Å). The GaO_4 tetrahedra in $BiGaO_3$ are joined by corners forming infinite $(GaO_3)^{3-}$ chains along the *a* axis. Bi^{3+} ions in $BiGaO_3$ have 6-fold coordination. Both $BiAlO_3$ and $BiGaO_3$ decompose at ambient pressure on heating above 820 K to give $Bi_2M_4O_9$ and $Bi_{25}MO_{39}$ (M = Al and Ga). Vibrational properties of $BiAlO_3$ and $BiGaO_3$ were studied by Raman spectroscopy. In solid solutions of $BiAl_{1-x}Ga_xO_3$, a *C*-centered monoclinic phase structurally related to $PbTiO_3$ with lattice parameters of $a = 5.1917(4)$ Å, $b = 5.1783(4)$ Å, $c = 4.4937(3)$ Å, and $\beta = 91.853(3)°$ was found.

1. Introduction

Bi- and Pb-containing perovskites with transition metals have received renewal attention in recent years due to the great interest in multiferroic materials.[1,2] In multiferroic systems, two or all three of the properties (anti)ferroelectricity, (anti)ferromagnetism, and ferroelasticity occur in the same phase. Such systems are rare in nature[3] but potentially with wide technological applications.[1,2,4] In the 1960s, Bi- and Pb-containing perovskites were also investigated a great deal as candidate multiferroic systems.[5−8]

Simple compounds, such as $BiCrO_3$,[8,9] $BiMnO_3$,[8,10,11] $BiFeO_3$,[12−14] $BiCoO_3$,[15] $BiNiO_3$,[16] and $PbVO_3$,[17,18] double perovskites, for example, Bi_2MnNiO_6[4] and $PbFe_{2/3}W_{1/3}O_3$,[5,19] and others were studied. Note that most of the above-mentioned simple perovskite-like compounds can be prepared only using a high-pressure technique.[6−11,15−18] However little is known about simple Bi-containing compounds $BiMO_3$ with nonmagnetic M ions (M = Al, Sc, Ga, and In). Recent theoretical studies of $BiAlO_3$ and $BiGaO_3$ predicted that they should be high-performance piezoelectrics and ferroelectrics

* To whom correspondence should be addressed: International Center for Young Scientists, National Institute for Materials Science, Namiki 1-1, Tsukuba, Ibaraki, 305-0044, Japan. E-mail: Alexei.BELIK@nims.go.jp. Tel: +81 (029) 851-3354 (ext. 8587). Fax: +81 (029) 860-4706.

† ICYS, NIMS.

‡ Institute of Materials Structure Science.

§ Research Reactor Institute.

|| AML, NIMS.

⊥ HVEMS, NIMS.

(1) Kimura, T.; Goto, T.; Shintani, H.; Ishizaka, K.; Arima, T.; Tokura, Y. *Nature* **2003**, *426*, 55.

(2) Hur, N.; Park, S.; Sharma, P. A.; Ahn, J. S.; Guha, S.; Cheong, S.-W. *Nature* **2004**, *429*, 392.

(3) Hill, N. A. *J. Phys. Chem. B* **2000**, *104*, 6694.

(4) Azuma, M.; Takata, K.; Saito, T.; Ishiwata, S.; Shimakawa, Y.; Takano, M. *J. Am. Chem. Soc.* **2005**, *127*, 8889.

(5) Smolenskii, G. A.; Chupis, I. E. *Sov. Phys. Usp.* **1982**, *25*, 475, and references therein.

(6) Tomashpol'skii, Y. Y.; Zubova, E. V.; Burdina, K. P.; Venevtsev, Y. N. *Inorg. Mater.* **1967**, *3*, 1861.

(7) Roth W. L.; DeVries, R. C. *J. Appl. Phys.* **1967**, *38*, 951.

(8) Sugawara, F.; Iiida, S.; Syono, Y.; Akimoto, S. *J. Phys. Soc. Jpn.* **1968**, *25*, 1553.

(9) Niitaka, S.; Azuma, M.; Takano, M.; Nishibori, E.; Takata, M.; Sakata, M. *Solid State Ionics* **2004**, *172*, 557.

(10) Kimura, T.; Kawamoto, S.; Yamada, I.; Azuma, M.; Takano, M.; Tokura, Y. *Phys. Rev. B* **2003**, *67*, 180401(R).

(11) (a) Montanari, E.; Righi, L.; Calestani, G.; Migliori, A.; Gilioli, E.; Bolzoni, F. *Chem. Mater.* **2005**, *17*, 1765. (b) Seshadri, R.; Hill, N. A. *Chem. Mater.* **2001**, *13*, 2892.

(12) Neaton, J. B.; Ederer, C.; Waghmare, U. V.; Spaldin, N. A.; Rabe, K. M. *Phys. Rev. B* **2005**, *71*, 014113 and references therein.

(13) Kubel, F.; Schmid, H. *Acta Crystallogr., Sect. B* **1990**, *46*, 698.

(14) Wang, J.; Neaton, J. B.; Zheng, H.; Nagarajan, V.; Ogale, S. B.; Liu, B.; Viehland, D.; Vaithyanathan, V.; Schlom, D. G.; Waghmare, U. V.; Spaldin, N. A.; Rabe, K. M.; Wuttig, M.; Ramesh, R. *Science* **2003**, *299*, 1719.

(15) (a) Niitaka, S.; Azuma, M.; Takano, M.; Nishibori, E.; Takata, M.; Sakata, M. *Meeting Abstracts of the Physical Society of Japan*, 59th Annual Meeting, March 27−30, 2004, Kyushu University; Vol. 59, Issue 1, Part 3, p 511 (ISSN 1342-8349). (b) Azuma, M.; Niitaka, S.; Belik, A. A.; Ishiwata, S.; Kanda, H.; Yamada, I.; Takano, M. *4th International Conference on Inorganic Materials*, Antwerp, Belgium, September 19−21, 2004, Book of Abstracts; Elsevier: Amsterdam, 2004; p 204.

(16) Ishiwata, S.; Azuma, M.; Takano, M.; Nishibori, E.; Takata, M.; Sakata, M.; Kato, K. *J. Mater. Chem.* **2002**, *12*, 3733.

(17) Shpanchenko, R. V.; Chernaya, V. V.; Tsirlin, A. A.; Chizhov, P. S.; Sklovsky, D. E.; Antipov, E. V.; Khlybov, E. P.; Pomjakushin, V.; Balagurov, A. M.; Medvedeva, J. E.; Kaul, E. E.; Geibel, C. *Chem. Mater.* **2004**, *16*, 3267.

(18) Belik, A. A.; Azuma, M.; Saito, T.; Shimakawa, Y.; Takano, M. *Chem. Mater.* **2005**, *17*, 269.

(19) Ivanov, S. A.; Eriksson, S. G.; Tellgren, R.; Rundlof, H. *Mater. Res. Bull.* **2004**, *39*, 2317.

10.1021/cm052020b CCC: $33.50
Published on Web 12/10/2005

with a very large spontaneous polarization.[20] Solid solutions including $BiMO_3$ as the end members, for example, $PbTiO_3-BiScO_3$ and $PbTiO_3-BiGaO_3$,[21−27] were extensively studied recently in attempts to improve ferroelectric properties of $PbTiO_3$ and reduce the amount of lead. Therefore, $BiMO_3$ with nonmagnetic M ions also seems to be interesting material.

Note that La-containing compounds $LaMO_3$ with nonmagnetic M ions are very important technological materials. $LaGaO_3$-based compounds are superior oxide-ion conductors.[28] $LaAlO_3$ is widely used as a substrate for thin-film growth of perovskite structures and structures containing perovskite-type blocks.[29] $LaScO_3$- and $LaInO_3$-based compounds are proton conductors.[30]

It is known that $BiScO_3$ can be prepared only at high pressure.[22,31] A triclinic perovskite-like cell was given for $BiScO_3$.[22,31] However, in the course of our studies of $BiMO_3$, we have shown that $BiScO_3$ has a monoclinic perovskite-like cell[32] and its structure is similar to multiferroic $BiCrO_3$,[9] $BiMnO_3$,[33] and Bi_2MnNiO_6.[4] The system $Bi_2O_3-Al_2O_3$ was investigated at ambient pressure.[34] The formation of $BiAlO_3$ was reported. However, no other information about $BiAlO_3$ was given and the authors failed to identify the existing compound ($Bi_{25}AlO_{39}$) in this system.[34] To our knowledge, there are no experimental reports on $BiGaO_3$ and $BiInO_3$. In the course of our studies, we have found that $BiInO_3$ has a perovskite $GdFeO_3$-type structure.[35]

In this work, we investigated $BiAlO_3$, $BiGaO_3$, and solid solutions $BiAl_{1-x}Ga_xO_3$ prepared at high pressure. Crystal structures of these compounds were studied by X-ray and time-of-flight neutron powder diffraction data. $BiAlO_3$ was found to be isotypic with the well-known multiferroic $BiFeO_3$, while $BiGaO_3$ has the structure closely related to that of KVO_3 with Ga^{3+} ions in tetrahedral coordination. The thermal stability and Raman spectra of $BiAlO_3$ and $BiGaO_3$ are also reported.

2. Experimental Section

2.1. Synthesis. Stoichiometric mixtures of Bi_2O_3, Al_2O_3, and Ga_2O_3 were pressed into pellets and annealed at 1023 K for 8 h. X-ray powder diffraction (XRD) showed that the resulting mixtures (precursors) consisted of Al_2O_3 and $Bi_{25}AlO_{39}$ for $BiAlO_3$ and $Bi_2Ga_4O_9$ and $Bi_{25}GaO_{39}$ for $BiGaO_3$. The precursors were placed in Au capsules and treated at 6 GPa in a belt-type high-pressure apparatus at 1273 K for 40 min for $BiAlO_3$ and at 1473 K for 15 min for $BiGaO_3$. After heat treatment, the samples were quenched to room temperature (RT), and the pressure was slowly released. $BiAlO_3$ was recovered from a Au capsule as a hard pellet, while $BiGaO_3$ was powder. $BiAlO_3$ was white with yellow tint, and $BiGaO_3$ was white. $BiAlO_3$ contained a small amount of unidentified impurities. $BiGaO_3$ contained a small amount of a new phase structurally related to $PbTiO_3$ (phase I, see section 3.5) and Ga_2O_3. Note that the high-pressure treatment of precursors instead of mixtures of oxides considerably reduced the amount of impurities, especially completely removed $Bi_2O_2CO_3$ as an impurity. The formation of $Bi_2O_2CO_3$ can be attributed to absorption of carbon-containing compounds (such as acetone, used for grinding, or CO_2) by Bi_2O_3. The appearance of carbon-containing impurities are often observed during high-pressure synthesis of Bi- and Pb-containing compounds, e.g., $BiMnO_3$[33] and $PbVO_3$.[17,18] For the preparation of $BiAl_{1-x}Ga_xO_3$ solid solutions with $x = 0.25$, 0.5, and 0.75, the stoichiometric mixtures of the precursors were treated at 6 GPa and 1373−1473 K for 30 min.

2.2. Thermal Analysis. The thermal stability of $BiAlO_3$ and $BiGaO_3$ was examined on a SII Exstar 6000 (TG-DTA 6200) system at a heating rate of 10 K/min between RT and 923 K. Differential scanning calorimetry (DSC) curves of $BiAlO_3$ and $BiGaO_3$ were recorded between 140 and 873 K at a heating rate of 10 K/min on a SII Exstar 6000 (DSC 6220) instrument in open aluminum capsules.

2.3. Vibrational Properties. Unpolarized Raman spectra of $BiAlO_3$ and $BiGaO_3$ were collected at RT with a micro Raman spectrometer (Horiba Jobin-Yvon T64000) in backscattering geometry with a liquid nitrogen cooled CCD detector. Raman scattering was excited using an Ar^+-Kr^+ laser at a wavelength of 514.5 nm. A 90× long working distance objective was used to focus the laser beam onto a spot of about 2 μm in diameter. The laser power on the $BiGaO_3$ sample was about 2 mW. $BiAlO_3$ was found to be damaged by this laser power. Therefore, the power was reduced about 5 times to collect the correct Raman spectrum of $BiAlO_3$.

2.4. XRD Experiments and Structure Refinements. XRD data of $BiAlO_3$ and $BiGaO_3$ were collected at RT on a Rigaku Ultima III diffractometer using Cu Kα radiation (2θ range of 21−151°, a step width of 0.02°, and a counting time of 20 s/step for $BiAlO_3$ and 2θ range of 15−145°, a step width of 0.02°, and a counting time of 11 s/step for $BiGaO_3$). The XRD data of $BiAlO_3$ were analyzed by the Rietveld method with RIETAN-2000.[36] Coefficients for analytical approximation to atomic scattering factors for Bi, Al, and O were taken from ref 37. The split pseudo-Voigt function

(20) Baettig, P.; Schelle, C. F.; LeSar, R.; Waghmare, U. V.; Spaldin, N. A. *Chem. Mater.* **2005**, *17*, 1376.
(21) Eitel, R. E.; Randall, C. A.; Shrout, T. R.; Rehrig, P. W.; Hackenberger, W.; Park, S. E. *Jpn. J. Appl. Phys. Part 1* **2001**, *40*, 5999.
(22) Inaguma, Y.; Miyaguchi, A.; Yoshida, M.; Katsumata, T.; Shimojo, Y.; Wang, R. P.; Sekiya, T. *J. Appl. Phys.* **2004**, *95*, 231.
(23) Cheng, J. R.; Zhu, W. Y.; Li, N.; Cross, L. E. *Mater. Lett.* **2003**, *57*, 2090.
(24) Cheng, J.; Eitel, R.; Li, N.; Cross, L. E. *J. Appl. Phys.* **2003**, *94*, 605.
(25) Eitel, R. E.; Zhang, S. J.; Shrout, T. R.; Randall, C. A.; Levin, I. *J. Appl. Phys.* **2004**, *96*, 2828.
(26) Zhang, S. J.; Randall, C. A.; Shrout, T. R. *Appl. Phys. Lett.* **2003**, *83*, 3150.
(27) Iniguez, J.; Vanderbilt, D.; Bellaiche, L. *Phys. Rev. B* **2003**, *67*, 224107.
(28) Kajitani, M.; Matsuda, M.; Hoshikawa, A.; Harjo, S.; Kamiyama, T.; Ishigaki, T.; Izumi, F.; Miyake, M. *Chem. Mater.* **2005**, *17*, 4235.
(29) Hayward, S. A.; Morrison, F. D.; T. Redfern, S. A.; Salje, E. K. H.; Scott, J. F.; Knight, K. S.; Tarantino, S.; Glazer, A. M.; Shuvaeva, V.; Daniel, P.; Zhang, M.; Carpenter, M. A. *Phys. Rev. B* **2005**, *72*, 054110.
(30) (a) Nomura, K.; Takeuchi, T.; Kamo, S.; Kageyama, H.; Miyazaki, Y. *Solid State Ionics* **2004**, *175*, 553. (b) Lybye, D.; Poulsen, F. W.; Mogensen, M. *Solid State Ionics* **2000**, *128*, 91. (c) Cheng, J. H.; Navrotsky, A. *J. Mater. Res.* **2003**, *18*, 2501.
(31) (a) Tomashpol'skii, Y. Y.; Venevtsev, Y. N. *Inorg. Mater.* **1969**, *5*, 1087. (b) Tomashpol'skii, Y. Y.; Zubova, E. V.; Burdina, K. P.; Venevtsev, Y. N. *Sov. Phys. Crystallogr.* (*Crystallogr. Rep.*) **1969**, *13*, 859. (c) Tomashpol'skii, Y. Y.; Venevtsev, Y. N. *Sov. Phys. Crystallogr.* (*Crystallogr. Rep.*) **1972**, *16*, 905.
(32) Belik, A. A.; Iikubo, S.; Kodama, K.; Igawa, N.; Shamoto, S.; Maie, M.; Nagai, T.; Matsui, Y.; Stefanovich, S. Yu.; Lazoryak, B. I.; Takayama-Muromachi, E. Submitted for publication.
(33) Atou, T.; Chiba, H.; Ohoyama, K.; Yamaguchi, Y.; Syono, Y. *J. Solid State Chem.* **1999**, *145*, 639.
(34) Speranskaya, E. I.; Skorikov, V. M.; Safronov, G. M.; Gaidukov, E. N. *Inorg. Mater.* **1970**, *6*, 1201.
(35) Belik, A. A.; Takayama-Muromachi, E. Unpublished results.
(36) Izumi, F.; Ikeda, T. *Mater. Sci. Forum* **2000**, *321−324*, 198.
(37) *International Tables for Crystallography*, Vol. C, 2nd ed.; Wilson, A. J. C., Prince, E., Eds.; Kluwer: Dordrecht, The Netherlands, 1999; pp 572−574.

of Toraya was used as a profile function.[38] The background was represented by a seventh-order Legendre polynomial. Isotropic atomic displacement parameters, U, with the isotropic Debye−Waller factor represented as $\exp((-8\pi^2 U \sin^2\theta)/\lambda^2)$ were assigned to all the sites. A 2θ region between 26° and 31.2° containing reflections of unknown impurities was excluded from the refinement in the case of $BiAlO_3$.

2.5. Time-of-Flight (TOF) Neutron Powder Diffraction Experiments and Structure Refinements. TOF neutron powder diffraction data of $BiGaO_3$ were measured at RT on the powder diffractometer Vega[39] ($\Delta d/d \approx 2 \times 10^{-3}$; d: spacing of lattice planes) at the pulsed spallation neutron facility KENS. About 5.0 g of the sample was contained in a V holder (diameter: 9.2 mm), which was slowly rotated during the measurement. An array of 160 position-sensitive detectors (PSDs) installed in a backward bank with a 2θ range from 150° to 170° was used to measure the intensity data. Incident neutron spectra were monitored with a ^{3}He monitor counter. Differences in efficiency between the PSDs and the monitor counter were corrected with intensity data resulting from a separate measurement of incoherent scattering from V. The experimental intensity data as a function of time were converted into those as a function of d, referring to data collected in a separate measurement of Si powder as a standard sample.

Neutron powder diffraction data in d ranges from 0.47 to 5.0 Å were analyzed by the Rietveld method with RIETAN-TN.[40] A composite background function, i.e., a 14th-order Legendre polynomial multiplied by a smoothed incident spectrum, was fit to the background. Bound coherent scattering lengths, b_c, used for the structure refinement were 8.532 fm (Bi), 7.288 fm (Ga), and 5.803 fm (O).[41]

For the impurity of Ga_2O_3, we refined only a scale factor and lattice parameters (a and c), fixing its structure parameters. The mass percentage of Ga_2O_3 in $BiGaO_3$ was calculated at 0.6% from the refined scale factors.

3. Results

3.1. Structure Refinement of $BiAlO_3$. Indexing Bragg reflections in the XRD data of $BiAlO_3$ revealed it to crystallize in the trigonal system with lattice parameters of $a \approx 5.375$ Å and $c \approx 13.393$ Å. Reflection conditions derived from the indexed reflections were $-h + k + l = 3n$ for hkl and $h + l = 3n$, $l = 2n$ for $h\bar{h}l$ (hexagonal axes, obverse setting), affording possible space groups $R3c$ (No. 161, noncentrosymmetric) and $R\bar{3}c$ (No. 167, centrosymmetric).[42] The XRD pattern of $BiAlO_3$ was found to be very similar to that of $BiFeO_3$. Therefore, for initial fractional coordinates in Rietveld analysis of $BiAlO_3$, we used those of $BiFeO_3$ with space group $R3c$.[43] When the structure was refined in space group $R\bar{3}c$,[29] the thermal parameter for the Al site (0, 0, 0) was 0.055(2) Å^2, and for the O site (x, 0, $^1/_4$) was 0.132(4) Å^2. This fact shows that the Al and O atoms are located off their special positions in the centrosymmetric structure. In addition, $BiAlO_3$ showed a second-harmonic generation signal about 150 times that of quartz, proving that $BiAlO_3$ crystallizes in the non-centrosymmetric space group.

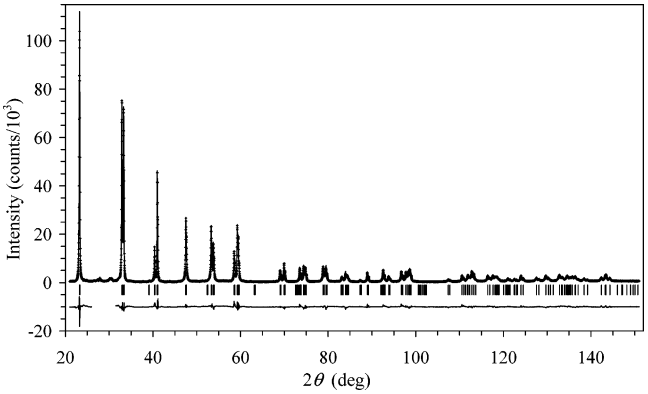

Figure 1. Observed (crosses) and calculated (solid line) XRD patterns for $BiAlO_3$. The difference pattern is shown at the bottom. The missing part on the difference pattern gives the region excluded from the refinement. Bragg reflections are indicated by tick marks.

Table 1. Structure Parameters Determined for $BiAlO_3$ from XRD Data[a]

site	Wyckoff position	x	y	z	$10^2 U$ (Å^2)
Bi[b]	6a	0	0	0	0.613(14)
Al	6a	0	0	0.2222(3)	0.15(9)
O	18b	0.5326(16)	0.0099(14)	0.9581(4)	0.6(3)

[a] Space group $R3c$ (No. 161); $Z = 6$; $a = 5.37546(5)$ Å, $c = 13.39334(14)$ Å, $V = 335.159(5)$ Å^3; $R_{wp} = 10.19\%$, $R_p = 6.98\%$, $R_B = 3.28\%$, $R_F = 2.49\%$, $S = R_{wp}/R_e = 4.30$. Occupancy factors of all the sites are unity. [b] The Bi site was placed at the origin ($z = 0$) owing to the arbitrariness of setting the origin in the non-centrosymmetric space group of $R3c$.

Table 2. Bond Lengths, l (Å), and Bond Valence Sums, BVS, in $BiAlO_3$ and $BiGaO_3$

$BiAlO_3$		$BiGaO_3$	
bonds	l	bonds	l
Bi−O (×3)	2.254(8)	Bi−O2 (×2)	2.157(2)
Bi−O (×3)	2.601(8)	Bi−O2 (×2)	2.290(2)
Bi−O (×3)	2.892(8)	Bi−O1 (×2)	2.705(2)
Bi−O (×3)	3.222(8)	BVS(Bi)	3.25
BVS(Bi)	3.20		
Al−O (×3)	1.853(7)	Ga−O2 (×2)	1.854(2)
Al−O (×3)	1.998(7)	Ga−O1 (×2)	1.860(2)
BVS(Al)	2.91	BVS(Ga)	2.84

Final lattice parameters, R factors, fractional coordinates, and U parameters for $BiAlO_3$ are listed in Table 1, and selected bond lengths, l, calculated with ORFFE[44] are listed in Table 2. Figure 1 displays observed, calculated, and difference XRD patterns.

3.2. Structure Refinement of $BiGaO_3$. Bragg reflections in the XRD pattern of $BiGaO_3$ could be indexed in an orthorhombic system with lattice parameters of $a \approx 5.4162$ Å, $b \approx 5.1335$ Å, and $c \approx 4.9685$ Å. For the indexing, we used TREOR.[45] A few very weak reflections were observed which could be indexed using the double c axis. These superlattice reflections were very strong in the TOF neutron diffraction pattern of $BiGaO_3$, indicating that their origin is the ordering of oxygen atoms. All reflections in the TOF

(38) Toraya, H. *J. Appl. Crystallogr.* **1990**, *23*, 485.
(39) Kamiyama, T.; Oikawa, K.; Tsuchiya, N.; Osawa, M.; Asano, H.; Watanabe, N.; Furusaka, M.; Satoh, S.; Fujikawa, I.; Ishigaki, T.; Izumi, F. *Physica B* **1995**, *213*−*214*, 875.
(40) Ohta, T.; Izumi, F.; Oikawa, K.; Kamiyama, T. *Physica B* **1997**, *234*−*236*, 1093.
(41) Sears, V. F. *International Tables for Crystallography*, 2nd ed.; Kluwer: Dordrecht, 1999; Vol. C, pp 440−450.
(42) *International Tables for Crystallography*, Vol. A, 5th ed.; Hahn, T., Ed.; Kluwer: Dordrecht, The Netherlands, 2002; p 52.
(43) Sosnowska, I.; Przenioslo, R.; Fischer, P.; Murashov, V. A. *J. Magn. Magn. Mater.* **1996**, *160*, 384.
(44) Busing, W. R.; Martin, K. O.; Levy H. A. *Report ORNL-TM-306*; Oak Ridge National Laboratory: Oak Ridge, TN, 1964.
(45) Werner, P. E.; Eriksson, L.; Westdahl, M. *J. Appl. Crystallogr.* **1985**, *18*, 367.

Table 3. Structure Parameters Determined for $BiGaO_3$ from TOF Neutron Diffraction Data[a]

site	Wyckoff position	*x*	*y*	*z*	$10^2 U_{eq}$ (Å^2)[b]
Bi	4d	1/4	0	0.6098(2)	0.81(5)
Ga	4e	1/4	1/2	0.3583(3)	0.22(5)
O1	4c	0	0.6333(4)	1/4	1.19(8)
O2	8f	0.9055(3)	0.2314(4)	0.0503(2)	0.78(5)

[a] Space group *Pcca* (No. 54); $Z = 4$; $a = 5.4162(2)$ Å, $b = 5.1335(3)$ Å, $c = 9.9369(5)$ Å, $V = 276.29(2)$ Å^3; $R_{wp} = 5.19\%$, $R_p = 3.65\%$, $R_B = 1.13\%$, $R_F = 0.82\%$, $S = R_{wp}/R_e = 4.18$. Occupancy factors of all the sites are unity. [b] $U_{eq} = (1/3)\sum_i\sum_j U_{ij}a_i^*a_j^*\mathbf{a}_i\mathbf{a}_j$.

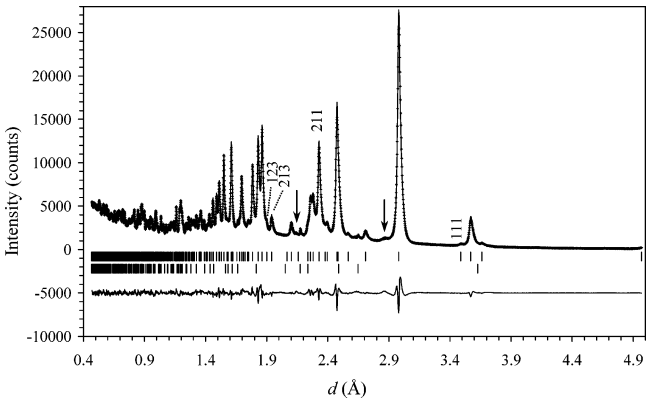

Figure 2. Observed (crosses), calculated (solid line), and difference patterns resulting from the Rietveld analysis of the TOF neutron powder diffraction data for $BiGaO_3$. Bragg reflections are indicated by tick marks. The lower tick marks are given for the impurity phase, Ga_2O_3. Indices of some reflections with $l = 2n + 1$ are given. Arrows are attached to reflections of a $PbTiO_3$-related phase (phase I).

neutron diffraction pattern could be indexed with lattice parameters of $a \approx 5.4162$ Å, $b \approx 5.1335$ Å, and $c \approx 9.9369$ Å. Reflection conditions derived from the indexed reflections in both XRD and TOF neutron diffraction patterns were $l = 2n$ for $0kl$, $h0l$, and $00l$ and $h = 2n$ for $hk0$ and $h00$, which leads to one possibility, the centrosymmetric space group *Pcca* (No. 54).[42]

The positions of Bi and Ga atoms and very approximate positions of O atoms in $BiGaO_3$ were determined ab initio by direct methods from the XRD data with EXPO[46] using the program's default settings. The positions of O atoms were then corrected using the geometrical parameters and located using the TOF neutron diffraction data. Finally, the structural parameters were refined by the Rietveld method from the TOF neutron diffraction data. In the last stage of the Rietveld refinement of $BiGaO_3$, we refined anisotropic atomic displacement parameters, U_{ij}, for all the sites.

Final lattice parameters, *R* factors, fractional coordinates, and U_{eq} parameters for $BiGaO_3$ are listed in Table 3, and selected bond lengths are listed in Table 2. U_{ij} parameters are given in the Supporting Information. Figure 2 displays observed, calculated, and difference TOF neutron diffraction patterns for $BiGaO_3$.

3.3. Thermal Stability of $BiAlO_3$ and $BiGaO_3$. Both DSC and DTA curves demonstrated a sharp exothermic peak centered at about 850 K for $BiAlO_3$ and $BiGaO_3$ (see Supporting Information). No other anomalies were observed

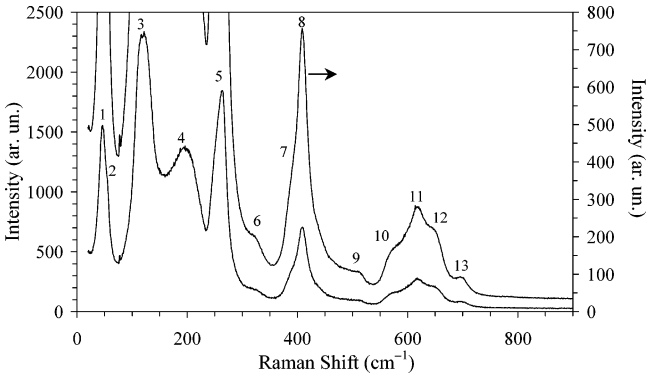

Figure 3. Raman spectrum of $BiAlO_3$ at RT. The enlarged Raman spectrum is present using the secondary axis. Numbers count the observed Raman bands. The list of wavenumbers of the bands appears in Table 4.

on the DSC curves from 140 to 873 K and on the DTA curves from 300 to 923 K. XRD data collected after the heating of the samples above 850 K showed that $BiAlO_3$ decomposed to a mixture of $Bi_2Al_4O_9$ and $Bi_{25}AlO_{39}$, and $BiGaO_3$ to a mixture of $Bi_2Ga_4O_9$ and $Bi_{25}GaO_{39}$. However, the phase composition of $BiAlO_3$ and $BiGaO_3$ heated to 723 K did not change. These facts indicated that both $BiAlO_3$ and $BiGaO_3$ decompose above 820 K and no structural phase transitions occur between 140 and 820 K.

The phase composition of the precursors and decomposed samples was different in the case of $BiAlO_3$, but the same in the case of $BiGaO_3$. Probably the synthesis temperature of 1023 K at ambient pressure was too low to reach equilibrium for the mixture of Bi_2O_3 and Al_2O_3 due to the low reactivity of Al_2O_3.

3.4. Raman Spectroscopy of $BiAlO_3$ and $BiGaO_3$. $BiAlO_3$ (space group C_{3v}^6) has two formula units in the primitive cell and therefore 30 degrees of vibrational freedom. Factor group analysis[47] predicts the following modes: $5A_1 + 5A_2 + 10E$. Of these, one A_1 and one E modes are the three acoustic modes, the five A_2 modes are Raman and infrared inactive, and the remaining $4A_1 + 9E$ optical modes are both Raman and infrared active. Therefore, 13 Raman active modes are expected without taking into account transverse and longitudinal splitting of the A_1 and E modes due to the non-centrosymmetric crystal structure. Experimentally (Figure 3), we observed all 13 modes whose wavenumbers are listed in Table 4.

$BiGaO_3$ (space group D_{2h}^8) has four formula units in the primitive cell and 60 degrees of vibrational freedom. Factor group analysis predicts the following modes: $6A_g + 7B_{1g} + 8B_{2g} + 9B_{3g} + 6A_u + 7B_{1u} + 8B_{2u} + 9B_{3u}$. The acoustic modes are $B_{1u} + B_{2u} + B_{3u}$. Raman active modes are A_g, B_{1g}, B_{2g}, and B_{3g}. Therefore, 30 Raman modes ($6A_g + 7B_{1g} + 8B_{2g} + 9B_{3g}$) are expected. We found 26 Raman modes experimentally (Figure 4 and Table 4).

3.5. Solid Solutions of $BiAl_{1-x}Ga_xO_3$. In the $BiAl_{1-x}Ga_xO_3$ solid solutions, the composition with $x = 0.75$ was almost single-phased with traces of phase I and $Bi_2O_2CO_3$. $BiAl_{0.25}Ga_{0.75}O_3$ adopted the $BiGaO_3$-type structure with lattice parameters of $a = 5.3923$ Å, $b = 5.1049$ Å, and $c = 9.918$

(46) Altomare, A.; Burla, M. C.; Camalli, M.; Carrozzini, B.; Cascarano, G. L.; Giacovazzo, C.; Guagliardi, A.; Moliterni, A. G. G.; Polidori, G.; Rizzi, R. *J. Appl. Crystallogr.* **1999**, *32*, 339.

(47) Rousseau, D. L.; Bauman, R. P.; Porto, S. P. S. *J. Raman Spectrosc.* **1981**, *10*, 253.

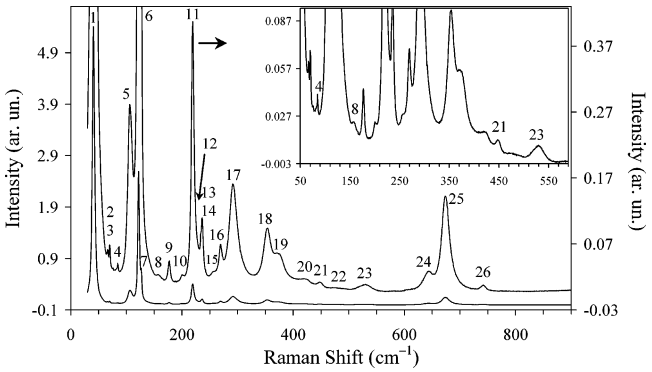

Figure 4. Raman spectrum of $BiGaO_3$ at RT. The enlarged Raman spectrum is present using the secondary axis and the inset. Numbers count the observed Raman bands. The list of wavenumbers of the bands appears in Table 4.

Table 4. Wavenumbers (cm^{-1}) of the Observed Raman Bands in $BiAlO_3$ and $BiGaO_3$

$BiAlO_3$		$BiGaO_3$	
no.	wavenumber	no.	wavenumber
1	46	1	42
2	55	2	67
3	120	3	71
4	197	4	84
5	264	5	107
6	322	6	123
7	391	7	126
8	411	8	158
9	512	9	178
10	574	10	203
11	617	11	220
12	651	12	226
13	699	13	234
		14	237
		15	256
		16	271
		17	294
		18	355
		19	375
		20	420
		21	450
		22	475
		23	531
		24	646
		25	675
		26	745

Å. These lattice parameters are smaller than those of $BiGaO_3$ in agreement with the smaller ionic radius of Al^{3+} (r_{IV} = 0.39 Å) compared with Ga^{3+} (r_{IV} = 0.47 Å) in tetrahedral coordination.[48] The sample with $x = 0.5$ contained a $BiGaO_3$-type phase with $a = 5.3692$ Å, $b = 5.0799$ Å, and $c = 9.901$ Å and a large amount of phase I. Because phase I can be considered as a quenched high-pressure high-temperature modification (see section 4), at least 50% of Al^{3+} can be substituted for Ga^{3+} in the tetrahedral site of $BiGaO_3$. The sample with $x = 0.25$ contained a $BiGaO_3$-type phase with $a = 5.3461$ Å, $b = 5.0620$ Å, and $c = 9.879$ Å, a $BiAlO_3$-type phase with $a = 5.4055$ Å and $c = 13.452$ Å, and a very large amount of phase I (see Supporting Information). The lattice parameters of the $BiAlO_3$-type phase in $BiAl_{0.75}Ga_{0.25}O_3$ were larger than those of $BiAlO_3$ ($a = 5.3755$ Å and $c = 13.3933$ Å). Because the ionic radius of Ga^{3+} (r_{VI} = 0.620 Å) in octahedral coordination is larger than that of Al^{3+} (r_{VI} = 0.535 Å),[48] this fact shows that a small amount of Ga^{3+} can replace Al^{3+} in the octahedral site of $BiAlO_3$.

(48) Shannon, R. D. *Acta Crystallogr., Sect. A* **1976**, *32*, 751.

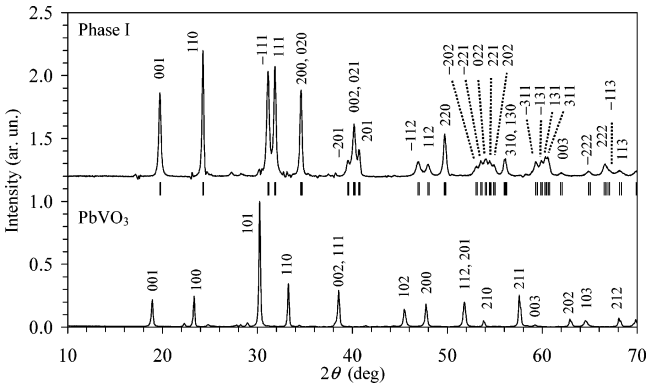

Figure 5. X-ray powder diffraction pattern of phase I in comparison with that of $PbVO_3$.[18] Indices of reflections are given in space group *Cm* (a = 5.1917 Å, b = 5.1783 Å, c = 4.4937 Å, and β = 91.853°) for phase I and *P4mm* (a = 3.8039 Å and c = 4.6768 Å) for $PbVO_3$. The XRD pattern of phase I was obtained by subtracting the calculated XRD patterns of the $BiGaO_3$- and $BiAlO_3$-type phases (after the Rietveld analysis) from the experimental XRD pattern of $BiAl_{0.75}Ga_{0.25}O_3$.

Octahedral and tetrahedral coordination is typical for both Al^{3+} and Ga^{3+} ions. Note that the $BiAl_{1-x}Ga_xO_3$ solid solutions were powder after high-pressure synthesis probably because of the presence of $BiGaO_3$-type phases.

Reflections of phase I in the sample with the nominal composition of $BiAl_{0.75}Ga_{0.25}O_3$ could be indexed with TREOR[45] in the *C*-centered monoclinic system with lattice parameters of a_I = 5.1917(4) Å, b_I = 5.1783(4) Å, c_I = 4.4937(3) Å, and β_I = 91.853(3)° (Figure 5). These lattice parameters resemble those of $PbVO_3$ (space group *P4mm*, a = 3.8039 Å $\approx a_I/\sqrt{2} \approx b_I/\sqrt{2}$ and c = 4.6768 Å $\approx c_I$), having the $PbTiO_3$-type structure.[18] An initial structure model for phase I was deduced from the structure parameters of $PbVO_3$ using the following sequence of transformations: *P4mm* → *Cmm2* → *Cm*. The subsequent Rietveld analysis of $BiAl_{0.75}Ga_{0.25}O_3$ gave reasonable bond lengths and R factors of R_B = 2.45% and R_F = 0.86% for phase I. These results show that the structure of phase I is closely related to that of $PbTiO_3$. However, the obtained structure parameters of phase I are preliminary because the exact composition of phase I is not known and because of the presence of a noticeable amount of the $BiGaO_3$- and $BiAlO_3$-type phases. The effective tetragonal distortion ($2\sqrt{2}c_I/(a_I + b_I)$) of phase I is 1.226.

4. Discussion

The crystal structure of $BiAlO_3$ could be successfully refined using the XRD data. $BiAlO_3$ crystallizes in a noncentrosymmetric perovksite-like structure. It is isotypic with multiferroic $BiFeO_3$ (space group *R3c*), in agreement with the theoretical prediction of the crystal structure of $BiAlO_3$.[20] The theoretically predicted lattice parameters are a = 3.84 Å (the parameter of the cubic perovksite) and α = 59.78° (rhombohedral axes). The experimental lattice parameters are $a = \sqrt{2} \times 3.8447$ Å and α = 59.25°. Al^{3+} ions occupy the site with octahedral coordination (Figure 6) and Bi^{3+} ions have 12 oxygen atoms in the first coordination sphere. The bond valence sums, BVS,[49] of the Bi and Al sites in $BiAlO_3$ calculated from the Bi−O and Al−O bond lengths are consistent with the formal oxidation states (Table 2).

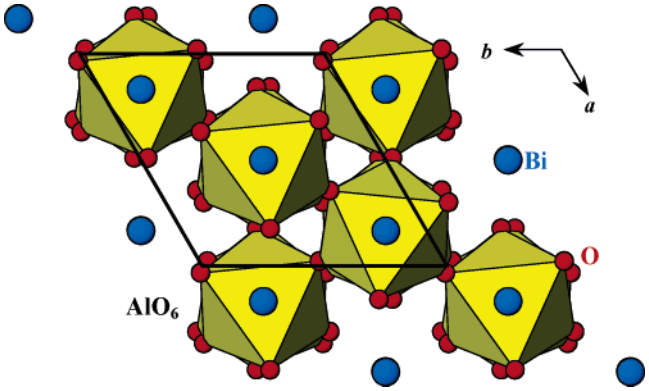

Figure 6. Schematic projection view of the structure of $BiAlO_3$ along the *c* axis. The AlO_6 octahedra are drawn. The Bi atoms are shown by circles.

The temperature of a ferroelectric-to-paraelectric phase transition in $BiAlO_3$ was predicted to be about 800 K.[20] However, $BiAlO_3$ starts to decompose around this temperature. Therefore, a ferroelectric-to-paraelectric phase transition in $BiAlO_3$ cannot be observed at ambient pressure in comparison to that in $BiFeO_3$, where the ferroelectric-to-paraelectric phase transition temperature is about 1120 K,[12] and the decomposition temperature is about 1200 K.[50]

$BiAlO_3$ is less distorted than $BiFeO_3$. In $BiAlO_3$, the Al^{3+} and O^{2-} ions are displaced by 0.37 and 0.56 Å, respectively, along the *c* axis from their ideal positions in a hypothetical structure with space group $R\bar{3}c$, while Fe^{3+} and O^{2-} ions in $BiFeO_3$ are displaced by 0.40 and 0.66 Å, respectively, along the *c* axis from their ideal positions.[43] Therefore, a spontaneous polarization calculated using the point-charge model[51] in $BiAlO_3$ (32 $\mu C/cm^2$) is smaller than that of $BiFeO_3$ (35 $\mu C/cm^2$). First-principles calculations of a polarization of $BiAlO_3$ and $BiFeO_3$ showed the same tendency.[12,20] The octahedral tilt angle (ω) of 5.5° in $BiAlO_3$ is also smaller than that of $BiFeO_3$ (12.3°).[52]

The crystal structure of $BiGaO_3$ could be successfully determined and refined only using the TOF neutron diffraction data because the *hkl* reflections with $l = 2n + 1$ were very weak on the XRD patterns (see Supporting Information). $BiGaO_3$ crystallizes in a centrosymmetric pyroxene-like structure. Ga^{3+} ions occupy the site with tetrahedral coordination. Bi^{3+} ions have six oxygen atoms in the first coordination sphere. The BVS values of the Bi and Ga sites in $BiGaO_3$ calculated from the Bi−O and Ga−O bond lengths are consistent with the formal oxidation states (Table 2). The GaO_4 tetrahedra are joined by corners with each other, forming the $(GaO_3)^{3-}$ infinite chains along the *a* axis (Figures 7a and 8a). $BiGaO_3$ has the structure closely related to that of the pyroxene-like KVO_3.[53] $BiGaO_3$ ($a_{BG} = 5.4162$ Å, $b_{BG} = 5.1335$ Å, and $c_{BG} = 9.9369$ Å) has lattice parameters similar to those of KVO_3 ($a = 5.176$ Å $\approx b_{BG}$, $b = 10.794$ Å $\approx c_{BG}$, and $c = 5.680$ Å $\approx a_{BG}$). However,

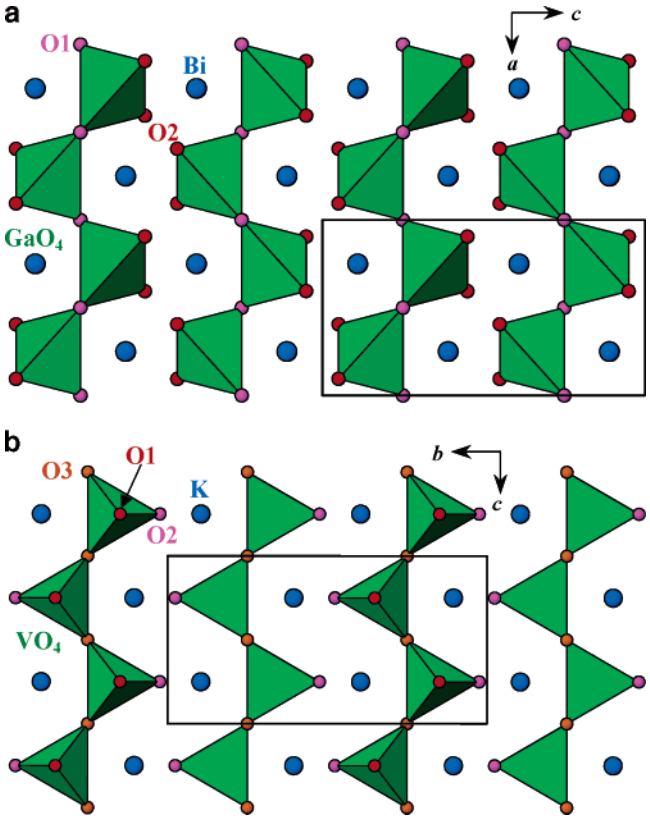

Figure 7. Schematic projection views of the structures of (a) $BiGaO_3$ along the *b* axis and (b) KVO_3 along the *a* axis. The GaO_4 and VO_4 tetrahedra are shown. The Bi and K atoms are given by circles.

$BiGaO_3$ crystallizes in space group *Pcca* (No. 54), while KVO_3 crystallizes in space group *Pbcm* (No. 57). The projections of the crystal structure of $BiGaO_3$ compared with those of KVO_3 are given in Figures 7 and 8. The VO_4 tetrahedra are faced up and down by the O1 atom if viewed along the *a* axis in KVO_3 (Figure 7b), while the GaO_4 tetrahedra in $BiGaO_3$ are tilted so that the GaO_4 tetradedra are faced up and down by the O1−O2 edge if viewed along the *b* axis in $BiGaO_3$ (Figure 7a). As a result, the coordination number of the large cation changes from 8 in KVO_3 to 6 in $BiGaO_3$.

In the theoretical prediction of the crystal structure of $BiGaO_3$, only perovskite-type structures were taken into account.[20] Among the perovskite-type structures, the tetragonal $PbTiO_3$-type structure with very large tetragonal distortion ($c/a = 1.3$) was found to have the lowest energy. In a hypothetical $PbTiO_3$-type structure, Ga^{3+} ions have a square-pyramidal coordination that is rather unusual for Ga^{3+} ions. Our experimental data showed that $BiGaO_3$ adopts the pyroxene-type structure with Ga^{3+} ions in a tetrahedral site that is typical for Ga^{3+} ions. Note that the tetragonal $PbTiO_3$-type structure was experimentally found in $PbVO_3$ ($c/a = 1.23$)[17,18] and $BiCoO_3$ ($c/a = 1.27$).[15] The fact that $BiGaO_3$ is obtained as powder after a high-pressure and high-temperature treatment suggests that a phase transition with a large volume change may occur in $BiGaO_3$ during the pressure (temperature) release as in the case of $PbVO_3$, where a simple cubic perovskite structure is stable at high pressure.[18] Therefore, structural investigations of $BiGaO_3$ under high pressure will be interesting. Note that pyroxenes are major

(49) Brese, R. E.; O'Keeffe, M. *Acta Crystallogr., Sect. B* **1991**, *47*, 192.
(50) Speranskaya, E. I.; Skorikov, V. M.; Rode, E. Y.; Terekhova, V. A. *Izv. Akad. Nauk SSSR, Ser. Khim.* **1965**, 905 (*Bull. Acad. Sci. USSR, Div. Chem. Sci. (Engl. Transl.)* **1965**, 873).
(51) Kwei, G. H.; Lawson, A. C.; Billinge, S. J. L.; Cheong, S.-W. *J. Phys. Chem.* **1993**, *97*, 2368.
(52) Beitollahi, A.; Thomas, N. W. *Acta Crystallogr., Sect. B* **1994**, *50*, 549.
(53) Hawthorne, F. C.; Calvo, C. *J. Solid State Chem.* **1977**, *22*, 157.

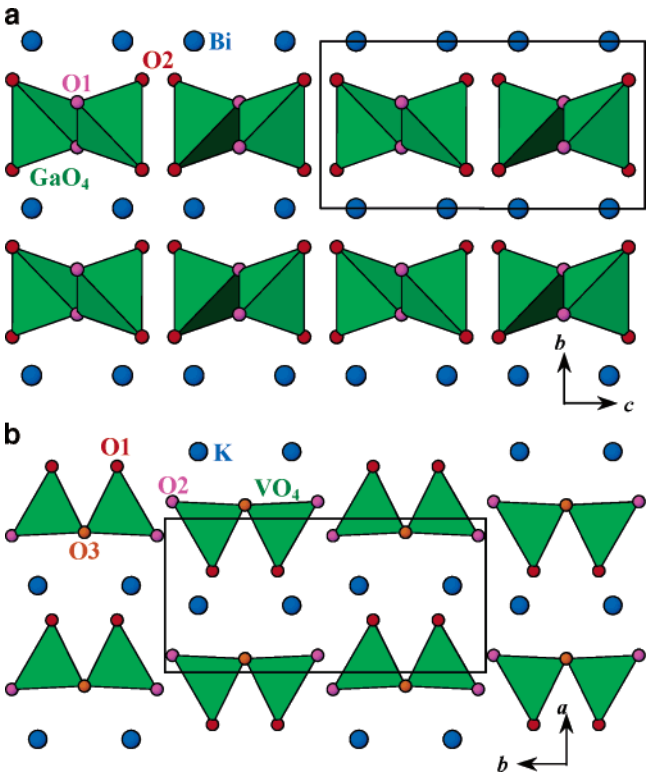

Figure 8. Schematic projection views of the structures of (a) $BiGaO_3$ along the *a* axis and (b) KVO_3 along the *c* axis. The GaO_4 and VO_4 tetrahedra are shown. The Bi and K atoms are given by circles.

components of the earth's crust and upper mantle and demonstrate various transformations under high pressure, e.g., in $MgSiO_3$[54] and $CuGeO_3$.[55]

The appearance of traces of phase I with a $PbTiO_3$-related structure in $BiGaO_3$ (Figure 2 and Supporting Information) supports the above idea about the phase transition under high pressure. The formation of phase I in a noticeable amount in the pseudo-binary system $BiGaO_3$−$BiAlO_3$ suggests nonequilibrium conditions. Under high pressure and high temperature, the $PbTiO_3$-related phase seems to be stable in $BiGaO_3$ and the $BiGaO_3$-rich side of the $BiAl_{1-x}Ga_xO_3$ solid solutions. However, phase I almost completely or partially transforms to the $BiGaO_3$-type phase during quenching to RT and release of pressure. Stabilization of the monophasic $PbTiO_3$-related phase in bulk or thin film appears to be very attractive as a lead-free ferroelectric or piezoelectric material.[20] Note that $BiFeO_3$ is stabilized in a $PbTiO_3$-related modification in thin film, while $BiFeO_3$ crystallizes in the trigonal system in bulk.[14]

In comparison to $BiGaO_3$, $LaGaO_3$ crystallizes at RT in a perovskite-type structure (the $GdFeO_3$-type structure with space group *Pnma*) with Ga^{3+} ions in an octahedral site.[28] $LaAlO_3$ also adopts a perovskite-type structure at RT. The lattice parameters of $LaAlO_3$ ($a = 5.3654$ Å and $c = 13.1126$ Å)[29] are similar to those of $BiAlO_3$ ($a = 5.3755$ Å and $c = 13.3933$ Å); however, $LaAlO_3$ crystallizes in the centrosymmetric space group $R\bar{3}c$. $LaScO_3$ and $LaInO_3$ also belong to the family of perovskite-type oxides.[30] Therefore, $BiGaO_3$ is unique among $BiMO_3$ because it crystallizes in the pyroxene-type structure at ambient pressure.

The Raman scattering technique is a sensitive tool for structural investigations. The number of observed Raman modes in $BiAlO_3$ is in agreement with the prediction confirming the *R*3*c* symmetry. Note that, to the best of our knowledge, there are no Raman studies on bulk multiferroic $BiFeO_3$ with the trigonal symmetry.[56] However, in $BiGaO_3$, we found only 26 Raman modes out of 30 expected ones. An assignment of the Raman lines to definite modes is not possible at present. The missing modes may have very low intensity, overlap with other modes, or be out of the spectral range (<20 cm^{-1}) of our Raman setup. The number of the expected modes in $BiGaO_3$ is large, which increases the probability of overlapping especially for powder samples (unpolarized Raman spectra). For example, in pyroxene-like $NaTiSi_2O_6$, 21 Raman modes were detected experimentally at RT out of 30 predicted modes.[57] On the other hand, all predicted 12 Raman modes were observed in pyroxene-like $CuGeO_3$.[55]

In conclusion, we prepared two new oxides $BiAlO_3$ and $BiGaO_3$, applying a high-pressure high-temperature technique. $BiAlO_3$ has a perovskite-type structure with Al^{3+} in an octahedral site, while $BiGaO_3$ adopts a pyroxene-type structure with Ga^{3+} in a tetrahedral site. Structure parameters of the two oxides were refined from X-ray and TOF neutron powder diffraction data. Thermal stability and vibrational properties of $BiAlO_3$ and $BiGaO_3$ were studied. In solid solutions of $BiAl_{1-x}Ga_xO_3$, a phase structurally related to $PbTiO_3$ was found.[58]

Acknowledgment. ICYS is supported by Special Coordination Funds for Promoting Science and Technology from MEXT, Japan. We thank Dr. S. Yu. Stefanovich of Moscow State University for the second-harmonic generation measurements and ICYS technical support staff for the assistance with TG-DTA, DSC, and Raman spectroscopy measurements.

Supporting Information Available: XRD patterns of $BiAl_{1-x}Ga_xO_3$ solid solutions with $x = 0.25$, 0.5, 0.75, and 1 (Figure S1); DTA and DSC curves of $BiAlO_3$ and $BiGaO_3$ (Figure S2); details of the Raman spectrum of $BiGaO_3$ (Figure S3); conditions of the diffraction experiments and parts of refinement results for $BiAlO_3$ and $BiGaO_3$ (Table S1); U_{ij} parameters determined from the TOF neutron diffraction data of $BiGaO_3$ (Table S2) (PDF). This material is available free of charge via the Internet at http://pubs.acs.org.

CM052020B

(54) Angel, R. J.; Chopelas, A.; Ross, N. L. *Nature* **1992**, *358*, 322.
(55) van Loosdrecht, P. H. M.; Zeman, J.; Martinez, G.; Dhalenne, G.; Revcolevschi, A. *Phys. Rev. Lett.* **1997**, *78*, 487.
(56) Singh, M. K.; Ryu, S.; Jang, H. M. *Phys. Rev. B* **2005**, *72*, 132101.
(57) Popovic, Z. V.; Konstantinovic, M. J.; Popov, V. N.; Cantarero, A.; Dohcevic-Mitrovic, Z.; Isobe, M.; Ueda, Y. *Phys. Rev. B* **2005**, *71*, 224302.
(58) About $PbTiO_3$-related phases with *Cm* symmetry see (a) Cox, D. E.; Noheda, B.; Shirane, G. *Phys. Rev. B* **2005**, *71*, 134110. (b) Wu, Z. G.; Cohen, R. E. *Phys. Rev. Lett.* **2005**, *95*, 037601.